



Published in final edited form as:

*J Am Chem Soc.* 2010 December 22; 132(50): 17928–17932. doi:10.1021/ja108568g.

## Tunable Bifunctional Silyl Ether Cross-Linkers for the Design of Acid Sensitive Biomaterials

Matthew C. Parrott<sup>1,3,6</sup>, J. Chris Luft<sup>1,3,6</sup>, James D. Byrne<sup>1,3,6</sup>, John H. Fain<sup>1,3,6</sup>, Mary E. Napier<sup>1,3,6</sup>, and Joseph M. DeSimone<sup>1,2,3,4,5,6,7,8,\*</sup>

Departments of Chemistry and Pharmacology, Carolina Center of Cancer Nanotechnology Excellence, Institute for Advanced Materials, Institute for Nanomedicine and Lineberger Comprehensive Cancer Center, University of North Carolina, Chapel Hill, NC 27599; Department of Chemical and Biomolecular Engineering, North Carolina State University, Raleigh, NC 27695; and Sloan-Kettering Institute for Cancer Research, Memorial Sloan-Kettering Cancer Center, New York, NY 10021

### Abstract

Responsive polymeric biomaterials can be triggered to degrade using localized environments found *in vivo*. A limited number of biomaterials provide precise control over the rate of degradation, the release rate of entrapped cargo, and yield a material that is intrinsically non-toxic. Here we design non-toxic acid-sensitive biomaterials based on silyl ether chemistry. A host of silyl ether cross-linkers were synthesized and molded into relevant medical devices including Trojan horse particles, sutures, and stents. The resulting devices were engineered to degrade under acidic conditions known to exist in tumor tissue, inflammatory tissue, and within diseased cells. The implementation of silyl ether chemistry gave precise control over the rate of degradation, and depending upon the steric bulk around the silicon atom, afforded devices that could degrade over the course of hours, days, weeks, or months. These novel materials could be useful for numerous biomedical applications including drug-delivery, tissue repair, and general surgery.

### Introduction

Silyl ethers are one of the most widely used protecting groups in organic chemistry.<sup>1</sup> Their popularity can be attributed to their ability to modulate the rate of deprotection depending upon the substituents on the silicon atom. For instance, trimethyl silyl ether (TMS), triethyl silyl ether (TES), and triisopropyl silyl ether (TIPS) protecting groups have a relative stability to acid catalyzed hydrolysis of 1, 64, and 700,000 respectively.<sup>1</sup> By simply changing the substituents from methyl to ethyl to isopropyl one can alter the rate of deprotection by orders of magnitude. Additionally, silyl ethers provide precise control over the rate of deprotection, the mechanism of deprotection, and the overall stability of a material. This class of chemistries has remained relatively unnoticed outside of protecting

\*desimone@email.unc.edu.

<sup>1</sup>Department of Chemistry, University of North Carolina

<sup>2</sup>Department of Pharmacology, Eshelman School of Pharmacy, University of North Carolina

<sup>3</sup>Carolina Center of Cancer Nanotechnology Excellence, University of North Carolina

<sup>4</sup>Institute for Advanced Materials, University of North Carolina

<sup>5</sup>Institute for Nanomedicine, University of North Carolina

<sup>6</sup>Lineberger Comprehensive Cancer Center, University of North Carolina

<sup>7</sup>Department of Chemical and Biomolecular Engineering, North Carolina State University

<sup>8</sup>Sloan-Kettering Institute for Cancer Research, Memorial Sloan-Kettering Cancer Center

Supporting Information Available: Full experimental details and characterization for all compounds and particles. This material is available free of charge via the Internet at <http://pubs.acs.org>.

group strategies. A successful adaptation of silyl ether chemistry, however, would afford a wide range of materials programmed to degrade under specific conditions found *in vivo*.

Researchers have exploited *in vivo* reducing environments,<sup>2-4</sup> enzymes,<sup>5-7</sup> and pH gradients<sup>8-10</sup> to trigger the cleavage or degradation of biomaterials. Specifically, hydrazones,<sup>11</sup> trityls,<sup>12</sup> aconityls,<sup>13</sup> vinyl ethers,<sup>14</sup> poly(ketals),<sup>15,16</sup> acetals,<sup>17</sup> poly(ortho esters),<sup>18</sup> and thiopropionates<sup>19</sup> utilize naturally occurring pH gradients to catalyze degradation, but are limited by tunability, toxic byproducts, or meticulous, multi-step syntheses. Conversely, a silyl ether linkage can be formed in one simple step, the degradation byproducts are non-toxic, and the linkage can be designed to degrade at different rates by merely altering the substituent on the silicon atom.

One silyl ether linkage of interest is the bifunctional silyl ether (BSE). Bifunctional silyl ethers consist of a C-O-Si(R)<sub>2</sub>-O-C linkage, and are commonly used for the protection of 1,2 and 1,3 diols.<sup>20-22</sup> The less hindered dimethyl, diethyl and diisopropyl BSEs are exceedingly susceptible to acid catalyzed hydrolysis, and are typically avoided as protecting groups. Although this property is unfavorable for protection strategies, less-hindered BSEs provide the ideal characteristics for highly susceptible, acid sensitive biomaterials.

## Results and Discussion

We therefore set out to prepare a collection of BSE cross-linkers with a variety of substituents on the silicon atom. The production of the desired cross-linkers utilized commercially available starting materials and required only one synthetic step, which proved to be inexpensive, rapid, and facile. Two similar silyl ether reactions (Scheme 1A and 1B) provided four novel, photopolymerizable cross-linkers denoted as **1**, **2**, **3** and **4**. For simplicity, we refer to the different cross-linkers according to the substituents on the silicon atom. For example, the cross-linker with two methyl substituents is referred to as dimethyl silyl ether or DMS, and the cross-linker with two ethyl substituents is referred to as diethyl silyl ether or DES.

Each cross-linker was molded into “Trojan horse” microparticles using a particle fabrication process called Particle Replication In Non-wetting Templates (PRINT).<sup>23</sup> PRINT is a top-down approach used to manufacture microparticles<sup>24-26</sup> and nanoparticles<sup>27-29</sup> with well defined size and shape. Two particle shapes were fabricated, 5  $\mu\text{m}$  cube particles (Figure 1A and 1B), and 3  $\mu\text{m}$  hexnut particles (Figure 2C and 2D) (full particle characterization can be seen in the supporting information). The microparticles were successfully prepared with each BSE cross-linker and were degraded under acidic conditions known to exist inside various cellular compartments.<sup>9</sup> The larger 5  $\mu\text{m}$  cube particles were employed to determine the rate of particle degradation at simulated lysosomal, endosomal, and physiological pH, or pH 5.0, 6.0, and 7.4 respectively.<sup>9</sup> A quantitative analysis of particle degradation was carried out on particles fabricated from DMS (**1**), DES (**2**), and DIS (**3**) cross-linkers, and loaded with 2 weight percent rhodamine-B. The particles were degraded and aliquots of the supernatant were removed, filtered, and the concentration of rhodamine-B was measured using UV spectroscopy. For accuracy, this experiment was repeated three times and the average data was fit to an exponential growth model to determine degradation half-lives.

A plot of rhodamine-B release versus time for particles fabricated with the DMS cross-linker (Figure 2A) displayed an accelerated rate of degradation when dispersed in a medium buffered at pH 5.0, and exhibited a degradation half life of 0.091 days or 2.19 hours (Table 1). The same particles dispersed in a medium buffered at pH 6.0 had a half life of 1.08 days, and particles dispersed in a medium buffered at pH 7.4 had a half life of 2.94 days. From this data it was apparent that the particles fabricated from the DMS cross-linker

preferentially degraded under acidic conditions, and the rate of degradation was accelerated as the pH decreased. Using identical conditions, particles fabricated with the DES cross-linker also degraded preferentially under acidic conditions (Figure 2B), but the rate of degradation was noticeably different. The DES particles appeared to degrade 13.6 times slower than the DMS particles when dispersed in a medium buffered at pH 5.0, and approximately 10 times slower when degraded in a medium buffered at pH 6.0 or pH 7.4. Furthermore, the rate of degradation of particles fabricated with the DIS cross-linker (Figure 2C) was slower by 2 orders of magnitude for all pH levels. This illustrates that by simply changing the substituent around the silicon atom one can effectively modulate the rate of particle degradation from hours to days to weeks to months.

Intracellular degradation of silyl ether PRINT particles could be visualized using transmission electron microscopy (TEM) and laser scanning confocal microscopy. We selected the hexnut shaped particles for this experiment due to their unique shape, which makes them easily distinguishable from cellular compartments. Two separate batches of hexnut particles were fabricated, one from the rapidly degrading DMS cross-linker, and one from the non degrading DTS cross-linker. A small amount of positively charged N-(3-aminopropyl)methacrylamide hydrochloride (APMA-HCl) was added to the composition to ensure a positive zeta potential and cellular internalization.<sup>30</sup> The transmission electron micrographs were captured in bright-field mode, which allows less dense material to appear white and highly dense material to appear dark.<sup>31</sup> Particles fabricated with the rapidly degrading DMS cross-linker can be seen in Figure 3A, where one DMS-hexnut particle was internalized, and three DMS-hexnut particles remain outside of the HeLa cell. A closer look of the internalized particle (Figure 3B) showed a bright white mass resembling a hexnut particle. The bright white color signifies that the particle became less dense than the surrounding intracellular matrix, and significantly less dense than the same particles found outside of the cell. The non-internalized DMS-hexnut particles (Figure 3C) appeared to be completely intact, and the size and shape of the particles were found to be equivalent to the size and shape of the particles imaged by scanning electron microscopy. Additional micrographs were taken to monitor the course of the DMS-hexnut degradation, and the internalized hexnut particles always became less dense or bright white, they appeared to swell (Figure 3D), then fragment (Figure 3E), and finally undergo surface erosion (Figure 3F). Particles prepared with the non-degrading DTS cross-linker can be seen in Figures 3G and 3H. These particles were also internalized within HeLa cells (and hence exposed to an acidic environment) but due to the stability of the cross-linker, the particle was not susceptible to degradation. In addition, there was no noticeable change to the shape, size, or density of the DTS-hexnut particles internalized inside HeLa cells.

Further investigation of intracellular degradation of silyl ether particles was achieved utilizing laser confocal microscopy. Two particle types were fabricated; one containing the rapidly degrading DMS cross-linker with fluorescein-o-acrylate (green fluorescent dye), and another particle containing the non-degrading DTS cross-linker and methacryloxyethyl thiocarbonyl rhodamine-B (red fluorescent dye). HeLa cells were incubated for 24 h with both the rapidly degrading particles (green) and the non-degrading particles (red) (Figure 4). It was clear that after cellular internalization the non-degrading DTS particles appeared to maintain the same size and shape and were not altered by intercellular conditions. On the other hand, the degradable DMS particles exhibited a number of different characteristics including; enlargement or swelling, loss of the distinct hexnut shape, fragmentation, and complete degradation as illustrated by the diffuse green fluorescence found in Figure 4C.

Cell viability experiments were performed to determine if the degradation byproducts were toxic. This was accomplished by separately dosing all four silyl-ether hexnut-particles (DMS, DES, DIS, and DTS) onto both HeLa and SKOV3 cell lines. The cytotoxicity of each

particle was determined using the CellTiter-Glo<sup>®</sup> luminescent cell viability assay (Figure 5). All of the silyl ether PRINT particles dosed onto HeLa and SKOV3 cells showed minimal toxicity across a large concentration range. These assays suggested that the silyl ether chemistry is non-toxic and the degradation byproducts appeared to be well tolerated in cells.

The novelty of bifunctional silyl ether cross-linkers is not limited to particle-based drug delivery applications. Devices fabricated from silyl ether biomaterials could also be useful for tissue repair, and general surgery. Biodegradable, and bioabsorbable devices are routinely used in hospitals and are often made from a co-polymer of lactic acid and glycolic acid identified as poly(lactic-co-glycolic acid) or PLGA.<sup>32</sup> A device made from PLGA is susceptible to both acid catalyzed degradation and enzymatic degradation by esterases.<sup>33–35</sup> Due to variable levels of enzymes, PLGA can degrade at different rates in different patients.<sup>36</sup> To the best of our knowledge, an enzyme specific to the silyl ether linkage does not exist. Therefore, devices fabricated from silyl ether biomaterials should only be susceptible to an acid catalyzed mechanism, and consequently minimize patient to patient variability.

Rudimentary medical devices such as sutures and stents were manufactured from the silyl ether cross-linkers according to several different procedures. As shown in Figure 6A, a thin fiber of the DMS cross-linker was prepared with a small amount of rhodamine-B. The fiber was designed with a diameter of 0.3 mm and a length of 50 cm, and would be recognized as a class 2-0 USP suture. The fiber was cut and placed in media buffered at pH 5.0 and pH 7.4. Analogous to the PRINT particles, the rate of degradation of the DMS fiber was accelerated at pH 5.0. Furthermore, the fiber suspended in medium buffered at pH 7.4 remained unbroken and showed minimal release of the rhodamine-B cargo over the course of 4 hours.

Stent-like devices were also made using each silyl ether cross-linker (Figure 6B). Each stent had an outer diameter of 3 mm, an inner diameter of 2.5 mm, a thickness of 0.25 mm, and a length of 25 mm, analogous to the dimensions of a typical coronary stent. Each stent was placed in an acidic solution (pH 5.0) and allowed to degrade over the course of 3 days. After the experiment was completed the stent made from the rapidly degrading DMS cross-linker showed significant change in shape and morphology. The stent made from the DES cross-linker became swollen and opaque, indicating the onset of degradation, while the remaining DIS and DTS stents showed no change over the course of the experiment.

## Conclusions

Bifunctional silyl ether cross-linkers were investigated as a new biomedical material useful for drug delivery and degradable devices. Using one facile synthetic step, we were able to synthesize four cross-linkers from commercially available reagents. Each cross-linker was successfully integrated into the PRINT platform, and yielded Trojan horse particles for drug-delivery. The particles were degraded under 3 different pH environments and the rate of degradation was accelerated as the pH decreased. Interestingly, the rate of acid catalyzed hydrolysis could be altered by orders of magnitude by simply changing the substituents on the silicon atom. *In vitro* particle degradation was visualized using transmission electron microscopy and laser confocal spectroscopy, which highlighted preferential degradation of particles internalized inside cells. Preliminary *in vitro* cytotoxicity data suggested that these materials were well tolerated across a large concentration range in two cell lines. Furthermore, the silyl ether biomaterials were molded into two practical medical devices, and shown to preferentially degrade under reduced pH. The rational design and implementation of silyl ether chemistry provided a fast and simple approach to a host of acid sensitive biomaterials. Further development of this silyl ether chemistry could generate

numerous devices susceptible to acidic environments, and that could be useful in a vast number of applications.

## Supplementary Material

Refer to Web version on PubMed Central for supplementary material.

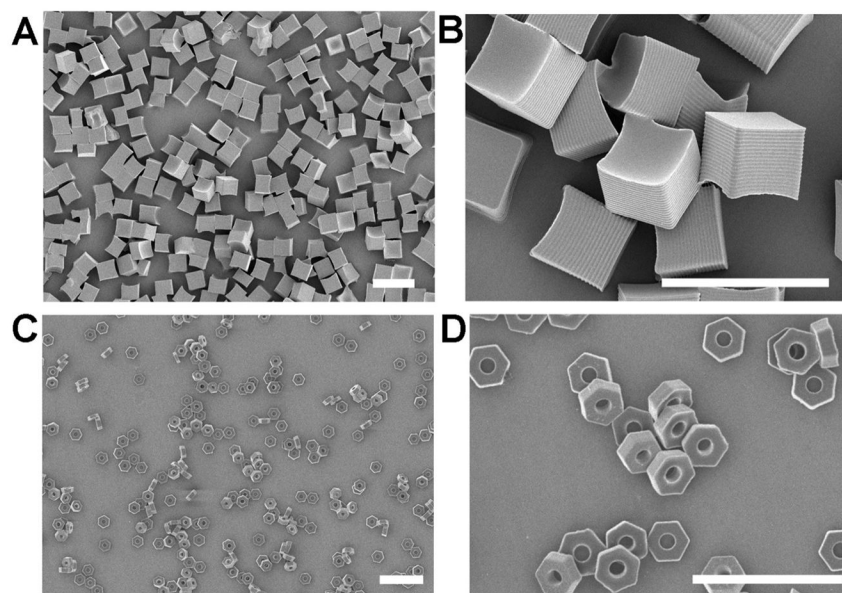
## Acknowledgments

The research was supported by the following; National Institutes of Health Grants 1R01EB009565-02, U54CA119373 (the Carolina Center of Cancer Nanotechnology), 1DP10D006432-01 (NIH Pioneer Award), the University Cancer Research Fund at the University of North Carolina at Chapel Hill, the William R. Kenan Professorship at the University of North Carolina at Chapel Hill, and a sponsored research agreement with Liquidia Technologies. We would also like to acknowledge Prof. Mark E. Davis for his helpful advice and discussions.

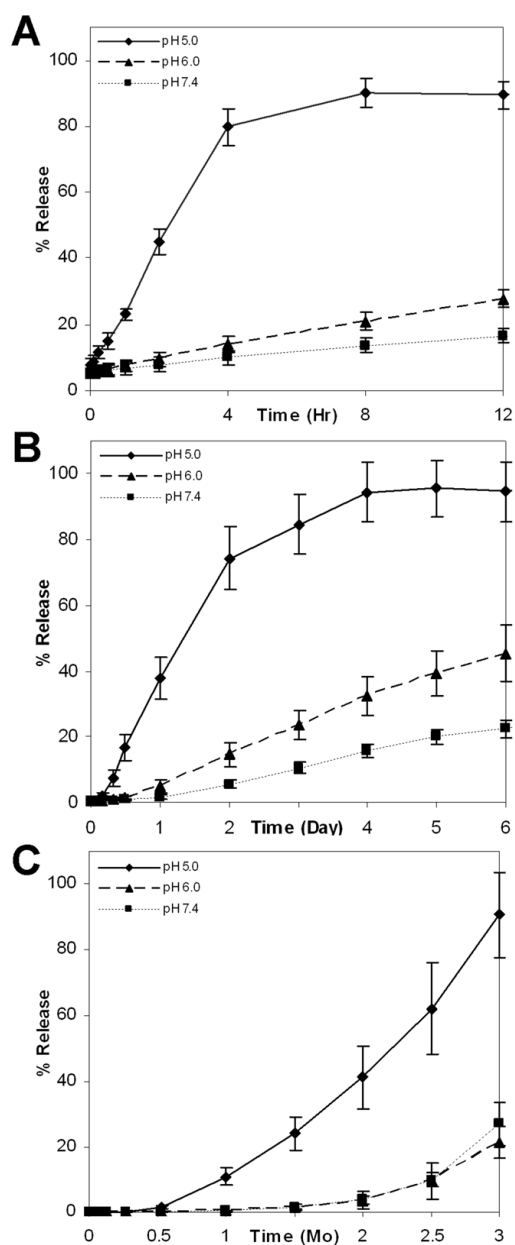
## References

1. Wuts, PGM.; Greene, TW. *Greene's Protective Groups in Organic Synthesis*. 4. Wiley; New York: 2007.
2. Bellomo G, Vairetti M, Stivala L, Mirabelli F, Richelmi P, Orrenius S. *Proceedings of the National Academy of Sciences of the United States of America*. 1992; 89:4412–4416. [PubMed: 1584774]
3. Jones DP, Carlson JL, Mody VC, Cai JY, Lynn MJ, Sternberg P. *Free Radical Biology and Medicine*. 2000; 28:625–635. [PubMed: 10719244]
4. Meister A. *Pharmacology & Therapeutics*. 1991; 51:155–194. [PubMed: 1784629]
5. Chau Y, Tan FE, Langer R. *Bioconjugate Chemistry*. 2004; 15:931–941. [PubMed: 15264885]
6. Mohamed MM, Sloane BF. *Nature Reviews Cancer*. 2006; 6:764–775.
7. Romberg B, Hennink WE, Storm G. *Pharmaceutical Research*. 2008; 25:55–71. [PubMed: 17551809]
8. Helmlinger G, Schell A, Dellian M, Forbes NS, Jain RK. *Clinical Cancer Research*. 2002; 8:1284–1291. [PubMed: 11948144]
9. Mellman I, Fuchs R, Helenius A. *Annual Review of Biochemistry*. 1986; 55:663–700.
10. Sun-Wada GH, Wada Y, Futai M. *Cell Structure and Function*. 2003; 28:455–463. [PubMed: 14745137]
11. Di Stefano G, Lanza M, Kratz F, Merina L, Fiume L. *European Journal of Pharmaceutical Sciences*. 2004; 23:393–397. [PubMed: 15567293]
12. Patel VF, Hardin JN, Mastro JM, Law KL, Zimmermann JL, Ehlhardt WJ, Woodland JM, Starling JJ. *Bioconjugate Chemistry*. 1996; 7:497–510. [PubMed: 8853464]
13. Shen WC, Ryser HJP. *Biochemical and Biophysical Research Communications*. 1981; 102:1048–1054. [PubMed: 7306187]
14. Shin J, Shum P, Thompson DH. *Journal of Controlled Release*. 2003; 91:187–200. [PubMed: 12932651]
15. Heffernan MJ, Murthy N. *Bioconjugate Chemistry*. 2005; 16:1340–1342. [PubMed: 16287226]
16. Sankaranarayanan J, Mahmoud EA, Kim G, Morachis JM, Almutairi A. *ACS Nano*. 2010; 4:5930–5936. [PubMed: 20828178]
17. Gillies ER, Frechet JMJ. *Bioconjugate Chemistry*. 2005; 16:361–368. [PubMed: 15769090]
18. Toncheva V, Schacht E, Ng SY, Barr J, Heller J. *Journal of Drug Targeting*. 2003; 11:345–353. [PubMed: 14668055]
19. Oishi M, Nagasaki Y, Itaka K, Nishiyama N, Kataoka K. *Journal of the American Chemical Society*. 2005; 127:1624–1625. [PubMed: 15700981]
20. Furusawa K, Katsura T. *Tetrahedron Letters*. 1985; 26:887–890.
21. Kumagai D, Miyazaki M, Nishimura SI. *Tetrahedron Letters*. 2001; 42:1953–1956.
22. Trost BM, Caldwell CG. *Tetrahedron Letters*. 1981; 22:4999–5002.

23. Rolland JP, Maynor BW, Euliss LE, Exner AE, Denison GM, DeSimone JM. *Journal of the American Chemical Society*. 2005; 127:10096–10100. [PubMed: 16011375]
24. Brown E, Forman NA, Orellana CS, Zhang HJ, Maynor BW, Betts DE, DeSimone JM, Jaeger HM. *Nature Materials*. 2010; 9:220–224.
25. Herlihy KP, Nunes J, DeSimone JM. *Langmuir*. 2008; 24:8421–8426. [PubMed: 18646784]
26. Nunes J, Herlihy KP, Mair L, Superfine R, DeSimone JM. *Nano Letters*. 2010; 10:1113–1119. [PubMed: 20334397]
27. Gratton SEA, Ropp PA, Pohlhaus PD, Luft JC, Madden VJ, Napier ME, DeSimone JM. *Proceedings of the National Academy of Sciences of the United States of America*. 2008; 105:11613–11618. [PubMed: 18697944]
28. Kelly JY, DeSimone JM. *Journal of the American Chemical Society*. 2008; 130:5438–5439. [PubMed: 18376832]
29. Petros RA, Ropp PA, DeSimone JM. *Journal of the American Chemical Society*. 2008; 130:5008–5009. [PubMed: 18355010]
30. Miller CR, Bondurant B, McLean SD, McGovern KA, O'Brien DF. *Biochemistry*. 1998; 37:12875–12883. [PubMed: 9737866]
31. Fultz, B.; Howe, JM. *Transmission Electron Microscopy and Diffractometry of Materials*. 3. Springer; New York: 2008.
32. Jagur-Grodzinski J. *Polymers for Advanced Technologies*. 2006; 17:395–418.
33. Chu CC, Williams DF. *Journal of Biomedical Materials Research*. 1983; 17:1029–1040. [PubMed: 6317694]
34. Parviainen M, Sand J, Harmoinen A, Kainulainen H, Valimaa T, Tormala P, Nordback I. *Pancreas*. 2000; 21:14–21. [PubMed: 10881928]
35. Williams DF, Mort E. *Journal of Bioengineering*. 1977; 1:231. [PubMed: 210160]
36. Davis, ME. Private Communication.

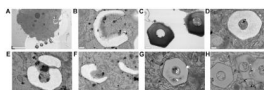


**Figure 1.** Scanning electron micrographs of 5  $\mu\text{m}$  cubes (1A, 1B) and 3  $\mu\text{m}$  hexnut particles (1C, 1D) fabricated using PRINT. (Scale bar: 10  $\mu\text{m}$ )

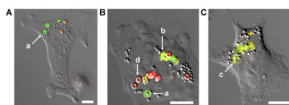


**Figure 2.** Percent rhodamine-B release versus time for 5  $\mu\text{m}$  cube particles fabricated from (A) DMS, (B) DES, and (C) DTS cross-linkers.

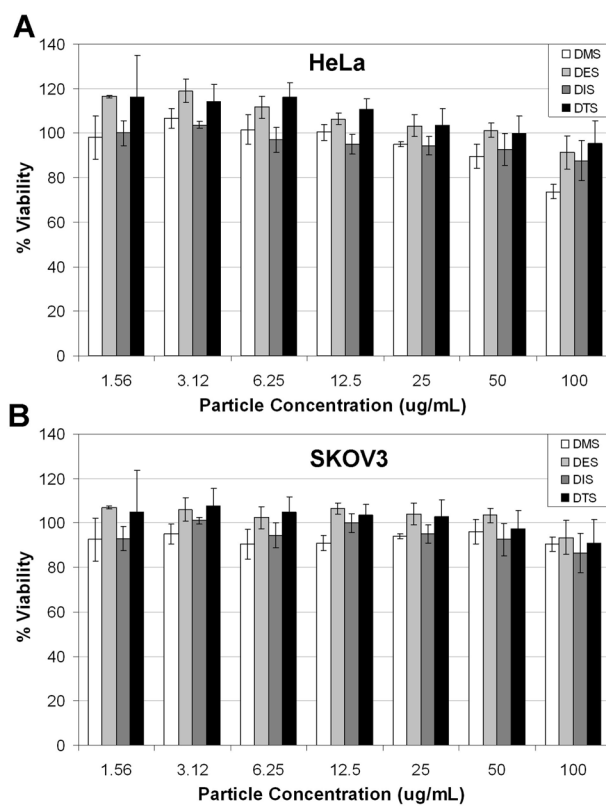




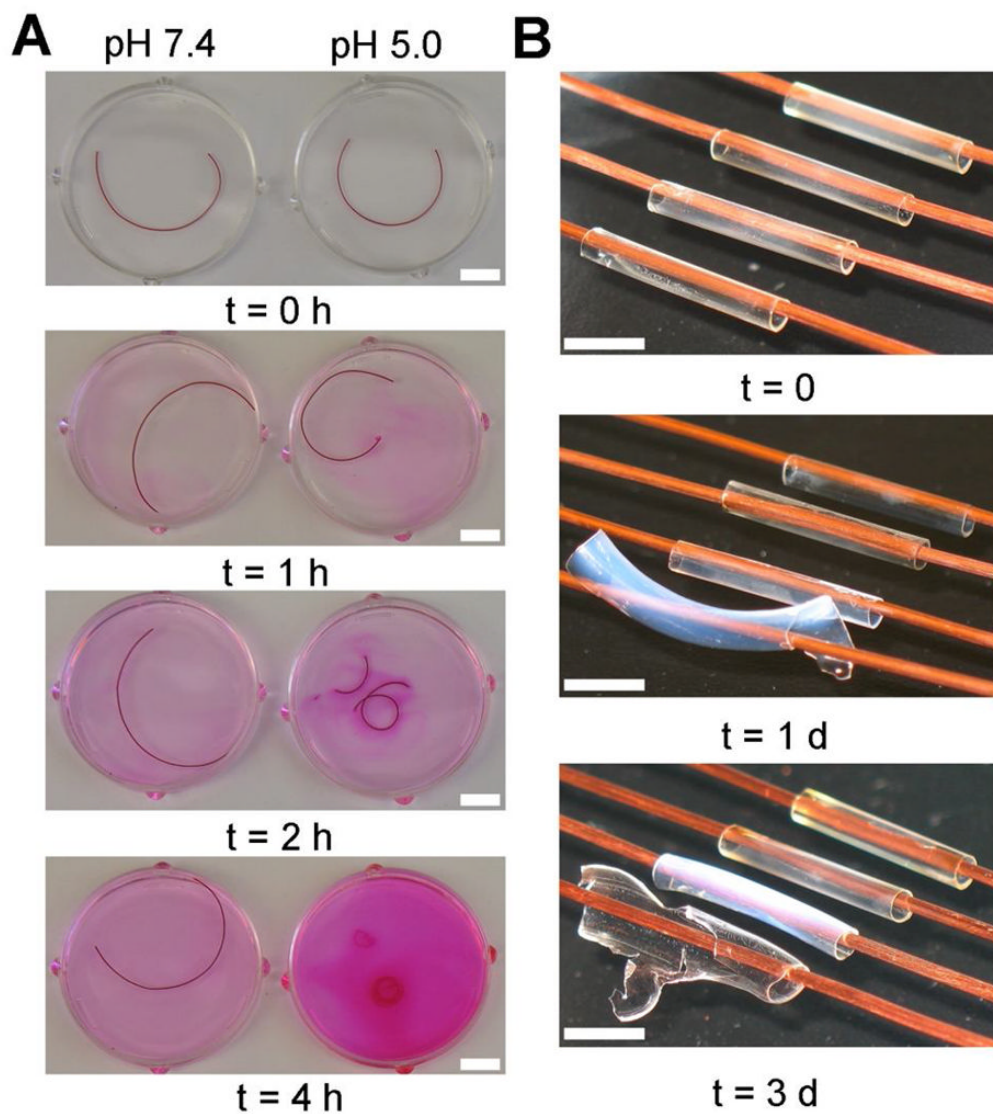
**Figure 3.** Transmission electron micrographs of PRINT hexnut particles incubated in HeLa cells. Rapidly degrading hexnut particles fabricated from the DMS crosslinker (A, scale bar: 10  $\mu\text{m}$  and B–F, scale bar: 0.5  $\mu\text{m}$ ), and non-degrading hexnut particles fabricated from the DTS crosslinker (G–H, scale bar: 0.5  $\mu\text{m}$ ).



**Figure 4.** Confocal laser scanning micrographs of HeLa cells incubated with rapidly degrading hexnut particles (green) and non-degrading hexnut particle (red). Micrographs highlight the phases of particle degradation: swelling (**a**), fragmentation (**b**), and complete degradation (**c**). The non-degradable particles showed no change when exposed to intracellular conditions (**d**) (scale bar: 10  $\mu\text{m}$ ).

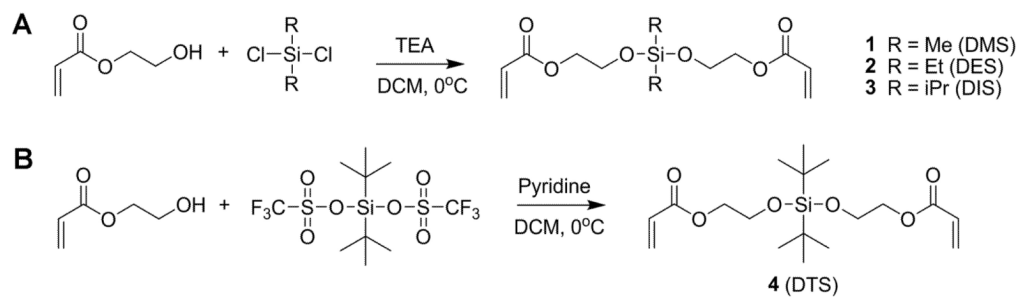


**Figure 5.** Cell viability assay (CellTiter-Glo<sup>®</sup>) of hexnut particles fabricated from DMS, DES, DIS and DTS crosslinkers. The assay was performed using HeLa (A) and SKOV3 (B).



**Figure 6. Biomedical devices fabricated from silyl ether crosslinkers**

**A**, A silyl ether suture fabricated from DMS and rhodamine-B was degraded in media buffered at pH 7.4 and pH 5.0 (scale bar: 1 cm). **B**, Silyl ether stents fabricated from compounds **1**, **2**, **3** and **4** (from left to right). Each stent was placed in a medium buffered at pH 5.0 and allowed to degrade (scale bar: 1 cm).

**Scheme 1.**

Synthesis of bifunctional silyl ether (BSE) cross-linkers.

**Table 1**

Degradation half life and normalized stability of 5  $\mu\text{m}$  silyl ether particles.

	DMS			DES			DIS		
pH	5.0	6.0	7.4	5.0	6.0	7.4	5.0	6.0	7.4
$T_{1/2}$ (day)	0.091	1.08	2.94	1.24	8.98	28.0	30.7	110	110
Norm.	1.00	11.8	32.3	13.6	98.7	308	337	1209	1209

Degradation data was imported into Origin and fit to an exponential growth curve. All  $R^2$  values were greater than 0.99.